N-linked glycosylation of native and recombinant cauliflower xyloglucan endotransglycosylase 16A

Hongbin HENRIKSSON*, Stuart E. DENMAN*, Iain D. G. CAMPUZANO†, Pia ADEMARK*, Emma R. MASTER*, Tuula T. TEERI* and Harry BRUMER, III*[1]

*Department of Biotechnology, Royal Institute of Technology (KTH), AlbaNova University Centre, 106 91 Stockholm, Sweden, and †Waters Corporation, Micromass MS Technologies, Atlas Park, Simonsway, Manchester M22 5PP, U.K.

The gene encoding a XET (xyloglucan endotransglycosylase) from cauliflower (*Brassica oleracea* var. *botrytis*) florets has been cloned and sequenced. Sequence analysis indicated a high degree of similarity to other XET enzymes belonging to glycosyl hydrolase family 16 (GH16). In addition to the conserved GH16 catalytic sequence motif EIDFE, there exists one potential N-linked glycosylation site, which is also highly conserved in XET enzymes from this family. Purification of the corresponding protein from extracts of cauliflower florets allowed the fractionation of a single, pure glycoform, which was analysed by MS techniques. Accurate protein mass determination following the enzymic deglycosylation of this glycoform indicated the presence of a high-mannose-type glycan of the general structure $GlcNAc_2Man_6$. LC/MS and MS/MS (tandem MS) analysis provided supporting evidence for this structure and confirmed that the glycosylation site (underlined) was situated close to the predicted catalytic residues in the conserved sequence YLSSTNNEHD-EIDFEFLGNRTGQPVILQTNVFTGGK. Heterologous expression in *Pichia pastoris* produced a range of protein glycoforms, which were, on average, more highly mannosylated than the purified native enzyme. This difference in glycosylation did not influence the apparent enzymic activity of the enzyme significantly. However, the removal of high-mannose glycosylation in recombinant cauliflower XET by endoglycosidase H, quantified by electrospray-ionization MS, caused a 40 % decrease in the transglycosylation activity of the enzyme. No hydrolytic activity was detected in native or heterologously expressed BobXET16A, even when almost completely deglycosylated.

Key words: glycoform, plant N-glycan, protein glycosylation, transglycosylation, xyloglucan endotransglycosylase (XET).

INTRODUCTION

Since the identification and initial characterization of XETs (xyloglucan endotransglycosylases; EC 2.4.1.207) more than a decade ago [1–6], these enzymes have received increasing attention due to their influence on plant cell growth and development. XET enzymes catalyse the cleavage and religation of xyloglucan, a hemicellulose composed of a $\beta(1 \rightarrow 4)$-linked glucan backbone, which contains $\alpha(1 \rightarrow 6)$-linked xylopyranose branches. The pattern of xylose substitution is quite regular; typically, groups of three xylosylated glucose residues are separated by one unsubstituted glucose residue. The xylopyranosyl residues may be substituted further by $\beta(1 \rightarrow 2)$-linked galactopyranosyl residues, which in turn may be derivatized with other monosaccharides, such as fucose or arabinose. The nature and extent of the substitution on the glucan chain is both species- and tissue-dependent [7,8]. In addition to acting as a predominant storage polysaccharide in the fruits of certain species such as *Tamarindus indica* (tamarind) and *Tropaeolum majus* (nasturtium), xyloglucan is found in a wide variety of plant tissues tightly associated with cellulose microfibrils through extensive hydrogen-bonding interactions. Xyloglucan appears to play a major role in maintaining the strength of the composite matrix that comprises the plant cell wall [9,10], as is indicated by the observation that enzymic depolymerization of xyloglucan leads to wall-softening phenomena such as fruit ripening [11,12].

In present models of cell wall expansion [13,14], a process which is driven by turgor pressure and which requires the deposition of nascent cell wall polysaccharides, the strength of the matrix must be compromised transiently to allow the cellulose microfibrils to move relative to each other. XET is believed to play a major role in this process due to its unique catalytic ability to cleave a xyloglucan chain endolytically and subsequently transfer the newly created chain end to the non-reducing end of a different xyloglucan molecule. A number of elegant studies have elucidated this general mechanism of XET acting upon xyloglucan *in vitro* [15–19], and XET activity has been demonstrated directly in plant tissues undergoing wall expansion [20,21] and restructuring [22–24]. Recent evidence also suggests that XET activity may play a role in strengthening the interaction between primary and developing secondary cell walls in wood-forming tissues [25].

The molecular biology of XET-related genes has been studied extensively across a wide range of plant species. Depending on the number of sequences analysed and the method of phylogenetic analysis employed, three to four sequence subfamilies have been identified [6,26–29], although the true functional significance of these subfamilies is unknown. All of the known XET-related genes are members of glycosyl hydrolase family 16 (GH16), which also contains a variety of endo-acting glucanases and galactanases (Carbohydrate-Active Enzymes server; http://afmb.cnrs-mrs.fr/CAZY/). It has been generally demonstrated that glycosidases within a family share similar three-dimensional

Abbreviations used: BCA, disodium 2,2′-bicinchoninate; DDA™, Data Directed Analysis™; Endo H, *Streptomyces plicatus* endoglycosidase H (EC 3.2.1.96); ESI, electrospray ionization; GH16, glycosyl hydrolase family 16; Gol, glucitol (in reduced oligosaccharides); MaxEnt™, Maximum Entropy™ algorithm; MS/MS, tandem MS; PNGase F, *Flavobacterium meningosepticum* N-glycosidase F (EC 3.5.1.52); RACE, rapid amplification of cDNA ends; TOF, time-of-flight; XET, xyloglucan endotransglycosylase; XGO, xyloglucan oligosaccharides; XTH, xyloglucan endotransglycosylase/hydrolase.

[1] To whom correspondence should be addressed (e-mail harry@biotech.kth.se).

The nucleotide sequence of *Brassica oleracea* var. *botrytis* XET16A has been submitted to the GenBank®, DDBJ, EMBL and GSDB Nucleotide Sequence Databases under the accession number AY156708.

structures and operate with the same stereochemical outcome of bond cleavage [30]. However, XET enzymes are mechanistically intriguing since, although they act through a double-displacement 'retaining' mechanism like their hydrolytic relatives, the active-site mechanism generally excludes water as an acceptor in the breakdown of the glycosyl–enzyme intermediate [31]. Instead, only xyloglucan itself or short XGO (xyloglucan oligosaccharides) are capable of acting as transglycosylation acceptors [16].

A significant hydrolytic activity has, however, been demonstrated for a small number of XET-related enzymes: the nasturtium *TmNXG1* gene product (subfamily III) [1], the kiwifruit (*Actinidia deliciosa*) *AdXET6* gene product (subfamily I) [32], and two adzuki bean (*Vigna angularis*) enzymes (gene sequences not determined) [33,34]. Native enzyme preparations from these sources are able to depolymerize high-molecular-mass xyloglucan in the absence of XGO acceptors. In light of these data, renaming this enzyme family as XTH (xyloglucan endotransglycosylase/hydrolase) has recently been proposed [35].

Cauliflower (*Brassica oleracea* var. *botrytis*) florets are a particularly rich source of XET, which is largely devoid of contaminating hydrolytic endo-xyloglucanase activity. Consequently, the XET isoenzymes from cauliflower have served as one of the primary models for studying the purification, protein biochemistry and enzymology of this unique enzyme class [17,18,36–39]. Despite this history, however, information about the molecular biology of cauliflower XET enzymes is presently unavailable.

More than 50 GH16 XET-related gene products have been studied to date. All but one contain a conserved potential N-linked glycosylation site, which is situated within 5–15 residues towards the C-terminus from the conserved GH16 active-site residues. Protein glycosylation has been demonstrated in the case of a native *Actinidia deliciosa* (kiwi fruit) XET [32] and, in two of four recombinant *Arabidopsis thaliana* XET enzymes, removal of N-linked glycosylation by enzymic treatment resulted in the near-total loss of transglycosylase activity [40,41]. Furthermore, X-ray crystallographic studies on *Populus tremula* × *tremuloides* XET expressed in *Pichia pastoris* reveal that N-linked glycosylation in that enzyme is situated on the acceptor side of the active-site cleft [42]. Despite their potential importance for catalytic activity, no information beyond that obtained by PNGase F (N-glycosidase F) treatment and SDS/PAGE analysis is available on the structure and composition of XET glycans from any source. Detailed glycosylation analysis could help to account for the observation of a number of cauliflower XET isoenzymes that can be fractionated on the basis of solubility in ammonium sulphate solutions of increasing concentration [17,39] or by isoelectric focusing [38].

To increase our understanding of the role of glycosylation in the catalytic activity of XET enzymes, we have used protein MS to elucidate the carbohydrate structure of a highly purified enzyme glycoform of cauliflower XET16A (BobXET16A; nomenclature according to [43]) that was purified from the native source. In addition, we have analysed the effects of protein glycosylation on the catalytic properties of the native and the heterologously expressed enzyme, and demonstrate how the accurate determination of intact glycoprotein masses can be used to rapidly determine the carbohydrate content of a mixture of glycoforms.

MATERIALS AND METHODS

General

Ultrapure water was used in all experiments, and refers to water purified on a Milli-Q® system (Millipore®) with a resistivity, ρ, of $\geqslant 18.2\ M\Omega \cdot cm$. Protein concentrations were determined by dye binding using the Bio-Rad® Protein Assay (Bio-Rad Laboratories, Hercules, CA, U.S.A.) with BSA as the standard. SDS/PAGE was performed using an XCell II™ Mini Cell (Novex, San Diego, CA, U.S.A.). Precast gels (NuPage; 4–12 %) were obtained from Novex, and marker proteins (LMW Calibration Kit) were from Amersham Biosciences. Proteins were visualized by silver staining [44]. N-terminal protein sequencing was performed by the Protein Analysis Centre at the Department of Medical Biochemistry and Biophysics, Karolinska Institute, Stockholm, Sweden, using repetitive Edman degradation on a protein sample that had been electroblotted on to a PVDF membrane following SDS/PAGE.

Enzyme substrates

Xyloglucan from tamarind seed was purchased from Megazyme (Bray, Ireland). XGO were prepared as follows. Xyloglucan (3 g) was dissolved in ultrapure water (200 ml) at 50 °C with vigorous stirring. Upon cooling to 30 °C, cellulase (30 mg, 4 units/mg; from *Trichoderma reesei*; Fluka) was added and the solution was maintained at that temperature overnight. Activated carbon (3 g) was then added, and the mixture was stirred for 15 min to adsorb the enzyme. Following the addition of acetonitrile (200 ml), the mixture was filtered through a pad of Celite on glass-fibre filter paper (Whatman GF/A). The filtrate was then concentrated *in vacuo* (water aspirator) and the residual solvent was removed by freeze-drying. This procedure produced a mixture of the oligosaccharides XXXG, XLXG, XXLG and XLLG in the molar proportions 15:7:32:46, as determined by HPAEC-PAD (high-performance anion-exchange chromatography with pulsed amperometric detection) [45]. {The nomenclature used is that of [46], where X represents a Xyl*p*(α1-6)-Glc*p* unit, L represents a Gal*p*(β1-2)Xyl*p*(α1-6)Glc*p* unit and G represents a Glc*p* residue. When written sequentially, a $\beta(1 \rightarrow 4)$ linkage between the Glc*p* residues is implied, with the reducing end on the right. Thus, written in IUPAC condensed notation, XLXG is Xyl*p*(α1-6)Glc*p*(β1-4)[Gal*p*(β1-2)Xyl*p*(α1-6)]Glc*p*(β1-4)[Xyl*p*(α1-6)]-Glc*p*(β1-4)Glc*p*. Gol represents glucitol in reduced oligosaccharides.} ESI (electrospray ionization)/MS analysis [Q-Tof™ (hybrid quadrupole-orthogonal TOF (time-of-flight) II; Waters Corp., Micromass MS Technologies, Manchester, U.K.] was used to confirm the identity of the oligosaccharides (results not shown). The mixture was sufficiently free of endoglucanase activity for use in the routine XET assays described below. When observed in overnight incubations, trace amounts of endoglucanase could be removed by passing XGO solutions through DEAE-Sepharose.

Purified XLLG was produced by HPLC fractionation on a TSKGel Amide-80 column (TosoHaas; 21.5 mm × 300 mm) using isocratic elution with an acetonitrile/water (11:9, v/v) mixture. Reduction of this material with $NaCNBH_3$ or $NaCNB^3H_3$ to produce XLLGol or [1-^{3}H]XLLGol respectively was performed essentially as described previously [39]. Following quenching of the reaction with acetic acid, the crude product was purified over a column of Bio-Gel P2 (1 cm × 10 cm; Bio-Rad; eluent: ultrapure water) to remove salts.

Colorimetric XET assay

An assay derived from that devised by Farkaš and co-workers [47] was used as follows. Enzyme (50 μl) was added to a solution composed of 50 μl of xyloglucan (2 mg/ml in ultrapure water), 50 μl of XGO (2 mg/ml in ultrapure water) and 50 μl of 200 mM citrate/phosphate buffer, pH 5.5, followed by incubation at 30 °C

for 30 min. To measure the contribution of substrate hydrolysis (endo-xyloglucanase activity) to the observed activity, control samples in which ultrapure water replaced the XGO mixture were measured in parallel. The reactions were terminated by adding 1 M HCl (100 μl). Immediately afterwards, 20 % Na_2SO_4 (800 μl) and potassium tri-iodide reagent (1 % KI and 0.5 % I_2 in ultrapure water; 200 μl) were added and the samples were allowed to stand in the dark for 30 min to allow colour development. For each sample, the change in absorbance at 620 nm per min is calculated relative to that in samples containing no enzyme [ΔA_{620}/min = ($A_{620}{}^{-\text{enzyme}}$/min) − ($A_{620}{}^{+\text{enzyme}}$/min)]. XET activity is expressed as the difference in ΔA_{620} per min between samples with and without the XGO mixture [$\Delta\Delta A_{620}$/min = ($\Delta A_{620}{}^{+\text{XGO}}$/min) − ($\Delta A_{620}{}^{-\text{XGO}}$/min)]. One unit of enzyme activity is defined as $\Delta\Delta A_{620}$/min = 1 min^{-1} in this assay.

Radioactive XET assay

The radioactive assay of Fry and co-workers [3,36,39] was adapted as follows, using 50 mM citrate/phosphate buffer, pH 5.5, as the assay buffer. [1-^{3}H]XLLGol was diluted with its non-radioactive isotopomer to produce a stock solution containing 2.2 mM XLLGol in buffer (specific radioactivity 3.7 TBq/mol). Appropriately diluted enzyme solution in buffer (10 μl) was added to a mixture of this [1-^{3}H]XLLGol stock solution (10 μl) and xyloglucan (10 μl; 3.0 g/l in buffer), followed by incubation at 25 °C for 30 min. The reaction was stopped by the addition of 50 % (v/v) formic acid in water (20 μl) and was dried on to Whatman 3MM chromatography paper circles (diameter 20 mm). The circles were washed for 4 h under running water, dried in an oven (65 °C), and analysed for incorporation of radioactivity in a Packard Tri-Carb 1500 scintillation counter by placing them flat on the bottom of scintillation vials followed by the addition of Ready-safe scintillation cocktail (6 ml; Beckman Coulter AB, Bromma, Sweden). There was no elution of radioactivity from the paper into the scintillation liquid. To account for non-specific adsorption of radioactivity on to the filter paper, samples where formic acid addition preceded enzyme addition were measured. Units of enzyme activity, expressed as nmol of XLLGol incorporated per min, were calculated from c.p.m. values using the specific radioactivity of XLLGol and a counting efficiency of 44 % for [^{3}H]xyloglucan [3]. One unit of enzyme activity is defined as 1 nmol of XLLGol incorporated/min in this assay.

Reducing sugar assay

The BCA (disodium 2,2′-bicinchoninate) reducing sugar assay of Garcia et al. [48] was adapted as follows. Recombinant BobXET16A (0.28 g/l) was incubated with or without xyloglucan (1 g/l) in 0.1 M sodium acetate, pH 5.5, at 30 °C. After 0, 30, 60, 120 and 240 min, 50 μl samples were withdrawn and diluted with ultrapure water (450 μl). Following the addition of BCA reagent (500 μl), the sample was heated at 80 °C for 30 min, cooled immediately on ice, and A_{560} was measured. Glucose was used to generate a seven-point standard curve over the concentration range 0–50 μM (0–25 nmol). All measurements were performed in duplicate.

pH–rate profile and thermal stability

The pH–rate profile of native cauliflower XET was determined over the pH range 4–8 using the colorimetric assay. The following buffers were used: 50 mM citrate/phosphate buffer (pH 4–6) and 50 mM phosphate buffer (pH 7–8). The thermal stability of native cauliflower XET was estimated by colorimetric measurement of XET activity in 50 mM citrate/phosphate buffer, pH 5.5, at temperatures ranging from 0 °C to 60 °C.

Purification of XET from cauliflower

Fresh cauliflower florets (500 g) were homogenized for 2 min in a household blender together with 750 ml of ice-cold extraction buffer (350 mM sodium citrate buffer containing 10 mM $CaCl_2$, pH 5.5). The extract was filtered through three layers of Miracloth (Calbiochem, San Diego, CA, U.S.A.) and then diluted 5-fold in water. SP-Sepharose Fast Flow gel (25 ml; Amersham Biosciences) was immediately added and adsorption was allowed to continue for 1 h at 4 °C with gentle stirring. The SP-Sepharose Fast Flow gel was collected and washed with 100 mM ammonium acetate buffer (pH 5.5) on a fritted glass filter funnel and then packed into a XK16/20 column (Amersham Biosciences). Proteins were eluted by a linear gradient of 0–1 M NaCl in 100 mM ammonium acetate, pH 5.5, over 10 column volumes. Fractions (4 ml) were collected at a flow rate of 2 ml/min. Those fractions showing the highest XET activity were pooled, mixed with an equal volume of 2 M $(NH_4)_2SO_4$ in 50 mM ammonium acetate, pH 5.5, and applied to a Resource ISO 1 ml column (Amersham Biosciences) that had been equilibrated previously with 1 M $(NH_4)_2SO_4$ in 50 mM ammonium acetate, pH 5.5. XET was eluted by a linear gradient of 1–0 M $(NH_4)_2SO_4$ (20 column volumes). All chromatographic steps were performed at room temperature.

Isolation of the gene encoding cauliflower XET16A

cDNA corresponding to the *BobXET16A* gene was isolated from total RNA extracts obtained by grinding fresh cauliflower florets (100 mg) with a mortar and pestle under liquid nitrogen, followed by processing using an RNeasy Plant Mini Kit (Qiagen, Hilden, Germany) according to the manufacturer's instructions. The XET cDNA was prepared using a '*C. therm*. Polymerase for Reverse Transcription in Two-Step RT-PCR kit' (Roche Diagnostics G.m.b.H., Mannheim, Germany) according to the manufacturer's protocol. The first strand of cDNA was synthesized using 1 μg of RNA and an oligo(dT)$_{18}$ primer with reverse transcriptase at 55 °C for 1 h. Degenerate nested primers for the specific PCR were designed based on N-terminal sequencing of the cauliflower XET protein, which indicated a sequence of IPPRKAIDVPFGRNY, and the conserved residues of the catalytic core of XET, i.e. EHDEIDFEFLGNRTG.

The sequences of all the primers used are shown in Table 1. The reverse primer CFXETR1 and the nested primer CFXETF1 were used in the second step of a nested PCR, resulting in a PCR product with the correct molecular mass and sequence corresponding to a XET fragment in the GH16 family. 5′ and 3′ RACE (rapid amplification of cDNA ends) were performed on 10 μg of total RNA using the First Choice RLM-RACE kit (Ambion, Austin, TX, U.S.A.), except that in the 5′ RACE reverse transcriptase step the random decamer primer was replaced with the 3′ RACE oligo(dT) primer. Nested PCRs were performed following the manufacturer's instructions using CFXET-5r-2 and CFXET-3r-2 (see Table 1) in the second PCR for the 5′ and 3′ RACE reactions respectively. The full-length cDNA was then amplified using a set of specific primers, CF-FL-F1 and CF-FL-R1, based on the 5′ and 3′ RACE sequence data. The nucleotide sequence of *Brassica oleracea* var. *botrytis* XET16A has been assigned GenBank accession number AY156708.

Table 1 Deoxynucleotide primers used for cloning *BobXET16A*

Name	Sequence
CFXETF1	AARGCNATHGAYGTNCCNTTYGG
CFXETF2	CCNCCNAGRAARGCNATHGAYGT
CFXETR1	AAYTCRAARTCDATYTCRTCRTGYTC
CFXET-5r-1	TGCAGTGACGACCCCAGCGGTATC
CFXET-5r-2	CAGCGGTATCACCAGCCGGCAG
CFXET-3r-1	CTGCCGGCTGGTGATACCGCTG
CFXET-3r-2	GATACCGCTGGGGTCGTCACTGCA
CF-FL-F1	AACATCATTCATCATCATCACCATCACC
CF-FL-R1	TGAACAGAAGCATAATACTCATAATAATCCGG
CFXET-f2-EM	TGACTACGTAATTCCTCCACGGAAAGC
CFXET-r3-EM	TTAGGCGGCCGCTCACACGTCTCTGTCCCTTCT

Production of cauliflower XET16A in *Pichia pastoris*

Full-length *BobXET16A* was PCR-amplified using a proofreading DNA polymerase (*Pfu*; Strategene) and the forward and reverse primers CFXET-f2-EM and CFXET-r3-EM respectively (Table 1). The amplified fragment was cloned into the *P. pastoris* expression vector pPIC9 (Invitrogen). DNA sequencing confirmed the identity of the expression construct, which was then transformed into *P. pastoris* GS115 cells by electroporation. Transformants were selected on media lacking histidine, and the presence of *BobXET16A* in transformants was confirmed by direct PCR amplification. Eight *P. pastoris* transformants were cultivated and induced to express BobXET16A according to the manufacturer's instructions (Invitrogen). Expression of active BobXET16A enzyme was confirmed by colorimetric XET activity assays and SDS/PAGE analysis of supernatant samples. For enzyme production, cells were grown in buffered glycerol/complex medium (BMGY; 20 ml) overnight at 30 °C and 200 rev./min. To induce BobXET16A expression, cells were harvested by centrifugation, resuspended in buffered methanol/complex medium (BMMY) to $D_{600} \approx 1$, then incubated at 22 °C and 200 rev./min for 3 days. Supernatant from 1 litre of a methanol-induced cultivation was filtered through a 0.45 μm-pore-size Versapor membrane (Pall Corp.) and concentrated by ultrafiltration. The culture medium was replaced by 100 mM sodium acetate, pH 5.5, and applied to a SP-Sepharose Fast Flow gel packed into a XK16/20 column (Amersham Biosciences). Proteins were eluted by a linear gradient of 0–1 M NaCl in 100 mM sodium acetate, pH 5.5, over 10 column volumes. Fractions (1 ml) were collected at a flow rate of 2 ml/min. Those fractions showing the highest XET activity were pooled, the buffer was replaced by 100 mM sodium acetate, and the sample was applied to a Resource S 1 ml column (Amersham Biosciences). XET was eluted by a linear gradient of 0–1 M NaCl in 100 mM sodium acetate, pH 5.5, over 20 column volumes. All chromatographic steps were performed at room temperature.

Protein deglycosylation by PNGase F

Protein deglycosylation with PNGase F for SDS/PAGE analysis was carried out under denaturing conditions using the N-Glycosidase F Protein Deglycosylation Kit (Roche) according to the manufacturer's instructions. Since the use of both ionic and non-ionic detergents in the kit precludes analysis by ESI/MS, samples were deglycosylated for this purpose without the use of detergents as follows. Native cauliflower XET (50 μl; 0.7 g/l in 0.1 M sodium acetate, pH 5.5, containing 0.5 M NaCl) was incubated with 10 μl (10 units) of PNGase F [Roche; in 50 mM sodium phosphate, 12.5 mM EDTA, 50 % (v/v) glycerol, pH 7.2] overnight at 37 °C. Prior to ESI/MS, buffer salts were removed by repeated concentration and dissolution in ultrapure water on centrifugal ultrafiltration membranes (Amicon YM-10; Millipore).

Digestion of XET and PNGase F-treated XET with trypsin

Proteolysis was performed by the direct addition of sequencing-grade trypsin (2 % by weight relative to XET) to samples of native and PNGase F-deglycosylated cauliflower XET without prior buffer exchange. Samples were incubated overnight at 37 °C.

Protein deglycosylation by Endo H (endoglycosidase H)

Prior to treatment of recombinant BobXET16A with Endo H (from *Streptomyces plicatus*; Roche), both enzymes were dialysed against 10 mM ammonium acetate (pH 5.5, adjusted with acetic acid) using Pierce Slide-A-Lyzer™ MINI flotation dialysis units (10–100 μl size; Boule Nordic AB, Huddinge, Sweden). Protein deglycosylation was carried out by adding dialysed Endo H (125 m-units; 25 μl) to XET protein (90 μg; 75 μl), followed by incubation at 25 °C. Samples for ESI/MS, activity assays and SDS/PAGE analysis were withdrawn at appropriate times during time-course experiments. In control samples, 10 mM ammonium acetate, pH 5.5, replaced the Endo H solution. To monitor XET activity during deglycosylation, the colorimetric assay was used as described above, except that the assay temperature was 25 °C and the assay time was shortened to 10 min. The calculation of the percentage of enzyme that was deglycosylated was based on the peak-area fraction of the deglycosylated XET after converting MaxEnt1 spectra (see Figure 8) into centroid spectra:

$$\text{Deglycosylation}(\%) = 100 \times (\text{area of peak } 32\,197)/(\text{sum of areas of peaks } 32\,197,\ 33\,697,\ 33\,859 \text{ and } 34\,021).$$

ESI/MS analysis: general

Mass spectrometric analysis was carried out on a Q-Tof™ II mass spectrometer fitted with a nano Z spray source (Waters Corp., Micromass MS Technologies). The instrument was operated at a resolution of $> 10\,000$ FWHM (full width at half maximum). Mass calibration was obtained over the range appropriate for each type of experiment using a solution of NaI (2 mg/ml) in propan-2-ol/water (1:1, v/v). Tryptic peptides were desalted by washing samples bound to a C18 ZipTip™ unit (Millipore) according to the manufacturer's instructions prior to elution with acetonitrile/water water (1:1, v/v) containing 0.1 % formic acid.

ESI/MS analysis of intact proteins

Intact proteins in ultrapure water or dilute volatile buffer solutions were diluted to 1–5 pmol/μl in acetonitrile/water (1:1, v/v) containing 0.1 % formic acid, and introduced into the mass spectrometer either by infusion through a nano Z spray source (syringe pump; 300–500 nl/min; source voltage ≈ 3000 V) or from borosilicate nanospray needles (source voltage 850 V). Data were typically acquired over the m/z range 400–2500 or 500–2000. The quadrupole mass filter of the Q-Tof™ II was operated in a wide band pass (RF only) mode when collecting TOF-MS data. The raw combined spectral data obtained were background subtracted and subjected to Maximum Entropy™ 1 deconvolution (Waters Corp., Micromass MS Technologies) to produce reconstructed zero-charge spectra.

Table 2 Purification of XET from cauliflower florets

XET was purified from 500 g of market-fresh cauliflower florets. In the radioactive assay, one unit is defined as 1 nmol of XLLGol incorporated/min. In the colorimetric assay, one unit is defined as $\Delta\Delta A_{620}/\text{min} = 1\ \text{min}^{-1}$. HIC, hydrophobic-interaction chromatography.

Step	Volume (ml)	Activity (units/ml)	Total activity (units)	Total protein (mg)	Specific activity (units/mg)	Yield (%)	Purification factor
Radioactive assay							
Extract	1000	20.5	20500	1400	14.6	100	(1)
Cation exchange	63	123	7740	52	149	38	10
HIC	7	174	1220	1.5	812	6	55
Colorimetric assay							
Extract	1000	0.27	270	1400	0.19	100	(1)
Cation exchange	63	2.6	160	52	3.1	59	16
HIC	7	5.8	41	1.5	27	15	140

LC/MS analysis of tryptic peptides

Tryptically digested samples were introduced into the mass spectrometer using a Waters Micromass® CapLC® System. A stream select module, attached directly to the nano Z spray source, was configured with a trapping column (0.3 mm × 5 mm; C18) where samples were loaded first via the autosampler and desalted. The 10-port valve was switched after aprrox. 3 min and a gradient [5–60 % (v/v) acetonitrile in aqueous 0.1 % formic acid] was run to elute the sample from the trap to the analytical column (C18 PepMap; 15 mm × 0.075 mm; LC Packings). A pre-column split gave a resultant flow though the column of 250 nl/min, with the pump delivering a flow of 2.5 μl/min.

DDA™ (Data Directed Analysis) was performed as follows. An initial TOF-MS survey scan was acquired over the mass range *m/z* 350–1600, with the criteria for MS to MS/MS (tandem MS) switching including ion intensity and charge state. The Q-Tof™ II was programmed to ignore singly charged ions and to perform MS/MS on up to four co-eluting species, with 1 s integration times. Switching back into MS survey mode was triggered after 4 s. The collision energy used to perform MS/MS was varied according to the mass and the charge state of the eluting peptide. Data for MS/MS were acquired over the mass range *m/z* 50–2000.

MaxEnt3™ (Maximum Entropy™ 3 algorithm) was used to simplify the raw combined spectral data obtained from the MS/MS fragmentation of each selected precursor ion. MaxEnt3 deconvolutes isotopic and charge state information in a continuum spectrum to generate a centroid spectrum containing only mono-isotopic, singly charged peaks, which both increases the apparent signal-to-noise ratio and facilitates spectral interpretation. *De novo* sequencing was performed using the MassLynx Software's PepSeq™ (Waters Corp., Micromass MS Technologies). Automated matching of interpreted MS/MS data from DDA™ experiments against the NCBInr database was performed via the internet using Mascot [49] at http://www.matrixscience.com/.

RESULTS

Purification of XET from cauliflower

A new method for the purification of cauliflower XET was devised, consisting of sequential cation-exchange and hydrophobic-interaction chromatography steps (Table 2). In the first step, the batch adsorption of XET from cauliflower extracts on to SP-Sepharose Fast Flow cation-exchange resin followed by collection of the resin on a coarse glass frit was found to assist greatly in the removal of extract debris that was otherwise difficult to separate by filtration through Miracloth or by centrifugation. Approx. 60 % of the XET activity (colorimetric assay) and less than 5 % of the total protein (Bradford assay) in the extract were captured during this batch adsorption process. Elution from the cation-exchange resin by an ammonium acetate gradient gave a broad peak of XET activity; on average, fifteen 5 ml fractions containing the highest XET activity were pooled for further fractionation. In the subsequent purification step on Resource ISO hydrophobic-interaction chromatography resin, XET activity was eluted as a sharp, single peak at approx. 0.5 M $(NH_4)_2SO_4$. Most of the contaminating protein (97 %) in the sample did not bind to the column and was collected in the flow-through fraction.

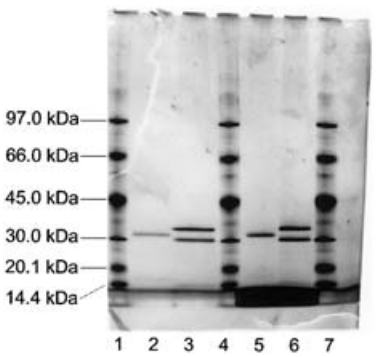

Figure 1 Silver-stained SDS/PAGE gel of purified native cauliflower XET

Lanes 1, 4, and 7, molecular-mass markers; lane 2, cauliflower XET (110 ng); lane 3, cauliflower XET (110 ng) treated with PNGase F (denaturing conditions); lane 5, cauliflower XET (220 ng); lane 6 cauliflower XET (220 ng) treated with PNGase F (denaturing conditions). The band of lower electrophoretic mobility (higher molecular mass) appearing in lanes 3 and 6 is PNGase F.

SDS/PAGE analysis of the pooled fractions obtained from the hydrophobic-interaction chromatography step showed a single, sharp band when visualized with silver staining, which shifted to a lower apparent molecular mass upon treatment with PNGase F (Figure 1). ESI/MS analysis yielded molecular masses for the native and deglycosylated samples of 33115 Da and 31737 Da respectively (see below).

Basic protein characterization of the purified XET enzyme was carried out in order to compare the protein obtained by the present method with cauliflower XET obtained in previous studies [17,39]. The pH optimum for this cauliflower XET is observed at approx. pH 5.5. Attempts to fit the observed pH–rate profile with a bell-shaped curve described by a model involving two ionizable active-site residues met with limited success (Figure 2A). While the decline in rate at high pH values is classically sigmoidal, that at low pH values is abrupt, and activity falls from 90 % of the maximal rate to nearly zero over one pH unit. The apparent pK_a values extracted from the curve-fitting procedure were 5.0 ± 0.3

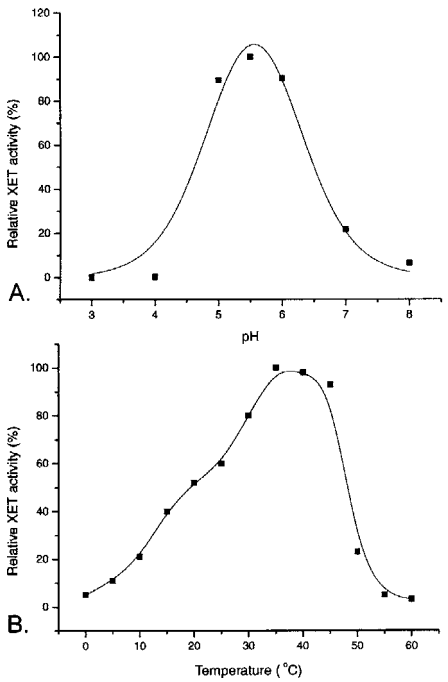

Figure 2 pH (A)– and temperature (B)–rate profiles of native cauliflower XET

(**A**) The curve represents the best fit to the expression $k_{obs} = k_{max}/[(1 + 10^{-pH}/10^{-pKa1})(1 + 10^{-pKa2}/10^{-pH})]$. (**B**) A B-spline curve was drawn through the data points using Microcal™ Origin® v.6.0 to serve as an ocular guide.

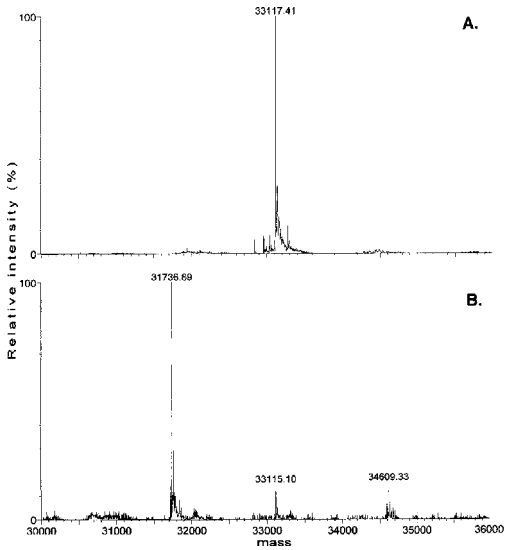

Figure 3 Reconstructed zero-charge spectra of native cauliflower XET (A) and PNGase F-treated cauliflower XET (B)

The peak at 36 409 Da in (**B**) is PNGase F.

and 6.1 ± 0.3. However, the poor fit of the curve ($r^2 = 0.971$; calculated $k_{max} = 167 \pm 56$), especially on the acidic limb, implies that these values should be viewed with some caution and may not represent true ionization constants of catalytically important amino acids.

The optimum temperature of the enzyme in the colorimetric XET assay was determined as a qualitative measure of protein stability. As shown in Figure 2(B), the transglycosylation ability of XET declines rapidly above 40 °C. This cauliflower XET also showed poor storage stability. Approx. 30 % of enzyme activity was lost during one freeze–thaw cycle and, when stored at 4 °C, a linear decline to zero activity was observed over 3 months [protein concentration ≈ 0.1 mg/ml in 50 mM ammonium acetate, pH 5.5, containing 0.5 M $(NH_4)_2SO_4$].

Heterologous expression of cauliflower BobXET16A

The yeast *P. pastoris* was found to be a suitable host for the production of active BobXET16A. Purification of the recombinant enzyme from the culture medium gave an electrophoretically homogeneous preparation (by SDS/PAGE), with a specific activity of 37 ± 2 units/mg (colorimetric assay). The overall yield was 2.4 mg/litre of culture medium, after purification.

Glycosylation and peptide analysis of native cauliflower XET by MS

Native cauliflower XET was nearly completely deglycosylated, as observed by ESI/MS, by treatment with PNGase F at 37 °C overnight in the absence of detergents. Background subtraction of combined individual mass spectra followed by MaxEnt1 processing gave the reconstructed spectra shown in Figure 3. The observed mass difference between the native XET (33 115 Da) and the PNGase F-treated XET (31 737 Da) was 1378 Da, which is consistent with the loss of an N-linked $GlcNAc_2Hex_6$ oligosaccharide. To confirm this observation and to localize the site of attachment of the glycan to the polypeptide backbone, a series of LC/MS and MS/MS experiments were undertaken on tryptic digests of the native and deglycosylated protein. In particular, we employed DDA™ experiments to aid in the identification of glycopeptides in crude tryptic digests of XET.

From DDA™ experiments, it was possible to identify a single glycopeptide by searching the MS/MS spectra for characteristic marker ions such as *m/z* 163 (protonated hexose residue $[Hex + H]^+$), *m/z* 204 (protonated *N*-acetylhexosamine residue $[HexNAc + H]^+$) or *m/z* 366 ($[HexHexNAc + H]^+$), which result from fragmentation of the glycan chain. Figure 4 shows the TOF-MS chromatogram, a single MS/MS chromatogram and a reconstructed ion chromatogram for the ions of *m/z* 163, 204 and 366 (generated from the MS/MS chromatogram) from a DDA™ experiment carried out on a tryptic digest of native cauliflower XET. The spectra constituting the major peak in the reconstructed chromatogram, which corresponded to MS/MS spectra of the triply charged ion of *m/z* 1260.2, were combined and subjected to MaxEnt3 deconvolution (Figure 5). The MaxEnt3 algorithm was used to simplify MS/MS spectra by deconvoluting charge-state and isotopic information to produce a spectrum containing only mono-isotopic, singly charged ions. From the high-mass region of the spectrum, six neutral losses of 162 Da and two neutral losses of 203 Da were clearly observed, which corresponded to the loss of hexose and *N*-acetylhexosamine residues respectively from the glycopeptide. The low-mass region of the spectrum corroborated this assignment; in addition to the ions of *m/z* 163, 204 and 366, which were first used to identify the glycopeptide, an ion series with six members whose masses are all separated by 162 Da was also observed extending towards higher *m/z* values from the *m/z* 204 ion. The observed fragment ions corresponded well to a glycan structure comprising an asparagine-linked $GlcNAc_2Hex_6$ oligosaccharide (where Hex is most likely to be mannose), which was postulated based upon the mass difference between the PNGase F-treated and untreated cauliflower XET.

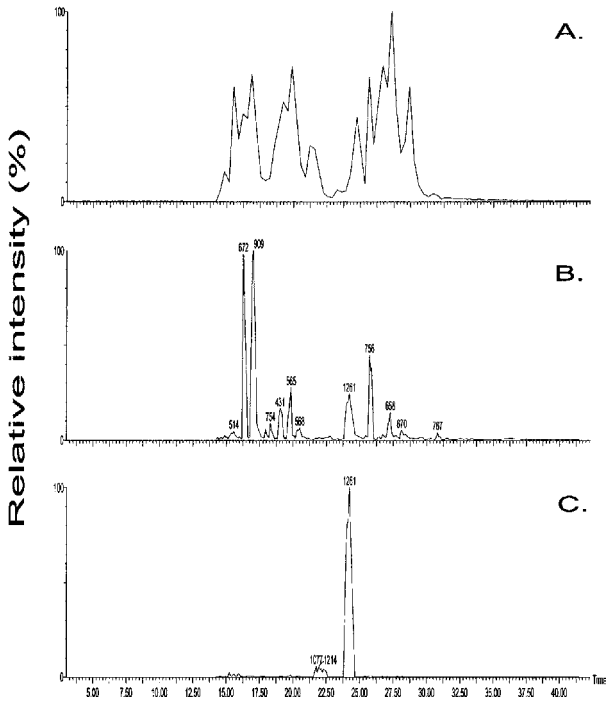

Figure 4 DDA LC-MS/MS analysis of a tryptic digest of native cauliflower XET

(**A**) TOF-MS survey; (**B**) single MS/MS component; (**C**) reconstructed ion chromatogram of spectra containing the ions *m/z* 163, 204 and 366.

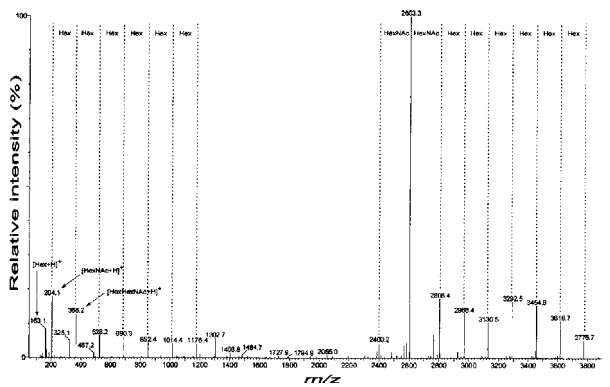

Figure 5 Deconvoluted spectrum obtained from MS/MS analysis of the triply charged glycopeptide ion of *m/z* 1260.2

The progressive neutral losses of hexose and *N*-acetylhexosamine have been annotated as Hex and HexNAc respectively.

Indeed, the base peak in the spectrum (*m/z* 2603) results from fragmentation of the glycosidic bond joining the two core GlcNAc residues in a process that is potentially assisted by anchimeric participation of the *N*-acetyl group. The weak ion intensity observed for the peptide fragment resulting from cleavage between the first GlcNAc unit and the Asn side chain may reflect the comparatively poor leaving group ability of the amide group.

Due to the lack of peptide bond fragmentation during MS/MS analysis of the glycopeptide, a tryptic digest of PNGase F-treated XET was analysed to identify the site of attachment of the glycan. Direct analysis of tryptic digests of cauliflower XET using

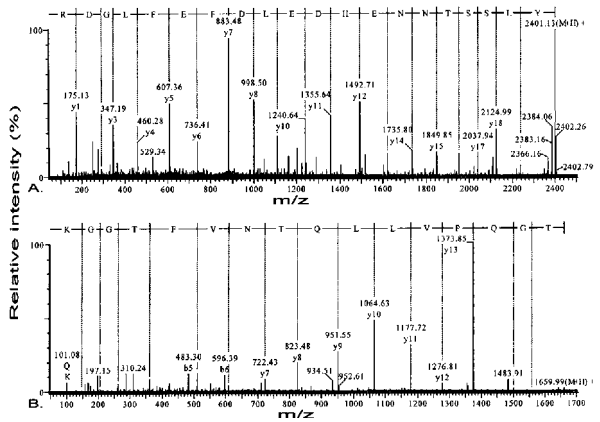

Figure 6 MS/MS sequence coverage of peptides spanning the N-linked glycosylation site of native cauliflower XET

(**A**) MaxEnt3-deconvoluted spectrum obtained from nanospray MS/MS analysis of the doubly charged precursor ion *m/z* 1201.0. (**B**) MaxEnt3-deconvoluted spectrum obtained from nanospray MS/MS of the doubly charged precursor ion *m/z* 830.47.

nanospray needles reconfirmed the presence of the triply charged ion of *m/z* 1260.2 in TOF-MS spectra of the native sample, while this ion was absent from spectra of the PNGase F-treated sample. Instead, two unique ions were observed from the latter sample at *m/z* 1201.0 (doubly charged) and *m/z* 801.0 (triply charged), both of which resulted from a peptide of 2400.0 Da. This value was identical with that expected for a peptide arising from PNGase F-catalysed deglycosylation of an N-linked $GlcNAc_2Hex_6$ moiety (1378.5 Da) from a 3777.5 Da glycopeptide. It should be noted that PNGase F (EC 3.5.1.52) is not actually a glycosidase, but an amidase that catalyses the removal of N-linked glycosylation by cleavage of the amide bond on the asparagine side chain. The resulting substitution of -OH for $-NH_2$ is responsible for the apparent 1 Da discrepancy between the calculated and observed deglycosylated peptide mass.

Both ions arising from the 2400.0 Da peptide yielded complete and identical sequence information when subjected to MS/MS analysis followed by MaxEnt3 deconvolution of combined individual spectra. The MaxEnt3 spectrum of the doubly charged *m/z* 1201.0 ion, which gives the sequence YLSSTNNEHDELDFEFLGDR (where L represents leucine or isoleucine), is shown in Figure 6(A). The peptide YLSSTNNEHDEIDFEFLGNR is found within the translated BobXET16A cDNA sequence (Figure 7). This peptide spans the predicted active-site motif and includes the first two residues of the predicted N-linked glycosylation site. The observation of aspartic acid in the mass spectrum, rather than the predicted asparagine, indicated that this residue was the site of attachment of an N-linked glycan released by PNGase F action.

The adjacent peptide towards the C-terminus within the BobXET16A sequence was also observed at *m/z* 830.47 (doubly charged) in the TOF-MS spectrum of trypsin-digested, deglycosylated cauliflower XET. MS/MS fragmentation of this ion gave complete sequence data, as shown in Figure 6(B). As with the preceding peptide, ambiguities in the MS/MS sequence due to isobaric Leu/Ile residues were resolved by comparison with cauliflower XET nucleotide sequence information to identify the peptide as TGQPVILQTNVFTGGK.

Careful analysis of all of the MS data obtained by TOF-MS analysis, manual MS/MS analysis and DDA™ combined with automated database searching allowed the identification of a large number of peptides arising from the tryptic digestion of native

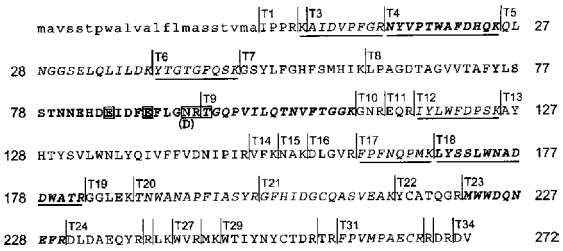

Figure 7 Complete translated cDNA sequence of cauliflower XET16A showing peptides identified by MS analysis

Sequence numbering begins at the first amino acid of the mature peptide. Labels T1–T34 denote predicted tryptic peptides. The predicted signal peptide is shown in lower-case letters. Boxed letters indicate the conserved GH16 catalytic glutamic acid residues (Glu-85 and Glu-89) and the conserved XET N-glycosylation motif. '(D)' at position 93 indicates the residue observed by MS/MS analysis of a PNGase F-treated sample. The method of peptide identification is denoted as follows: italics, TOF-MS mass match; bold, manual MS/MS analysis; underscore, automated Mascot database matching. Some peptides were identified by more than one technique, as indicated. Incompletely cleaved T2–3 and T5–6 peptides were also observed in TOF-MS spectra.

cauliflower XET. Figure 7 shows the translated peptide sequence of cauliflower XET16A derived from the complete cDNA sequence. Assignment of peaks in TOF-MS spectra was conservative; singly charged ions alone were not considered sufficient to identify a given peptide. The sequence coverage so obtained represented 61 % of the mature protein.

The calculated average mass of the mature cauliflower XET16A protein is 31737.95 Da, based on the cDNA sequence. Assuming the presence of two internal disulphide bonds as observed in the X-ray crystal structure of the related *Populus tremulous* × *tremuloides* XET16A [42] and the conversion of Asn-93 into Asp by PNGase F, the calculated mass is 31734.91 Da. This value corresponds well to the observed value (Figure 3B) of 31736.9 Da (64 p.p.m. error). These data, together with those obtained by MS peptide mapping and Edman N-terminal sequencing, strongly imply that the XET protein isolated from cauliflower florets is the translation product of the cloned BobXET16A cDNA.

Glycosylation analysis of recombinant BobXET16A expressed in *P. pastoris*, and effect of glycosylation on enzyme activity

ESI/MS was used to determine the glycosylation pattern of BobXET16A that had been produced heterologously in *P. pastoris*. Treatment with Endo H, which cleaves the $\beta(1 \rightarrow 4)$ glycosidic bond between the core GlcNAc monosaccharides in N-linked glycopeptides, over a period of 2 h resulted in the near complete deglycosylation of a mixture of peptide glycoforms to give a single peak in MaxEnt1-reconstructed spectra (Figure 8). The cloning strategy used to insert the *BobXET16A* gene into the expression vector resulted in the addition of the dipeptide Tyr-Val to the N-terminus of heterologously expressed BobXET16A. The calculated average mass for the resulting gene product, assuming the presence of two internal disulphide bonds and an N-linked GlcNAc residue, is 32199.3 Da. This value is in good agreement with the observed mass of the Endo H-deglycosylated enzyme of 32197 Da (Figure 8E), corresponding to an error of 71 p.p.m. The data in Figure 8 were obtained using an external mass calibration of the TOF detector prior to the experiment, and are therefore subject to temperature-dependent drift. It is in principle possible to use the Endo H peak as an internal standard to obtain higher mass accuracy; however, this is confounded by the observation in our laboratory that the protein mass of commercial (Roche)

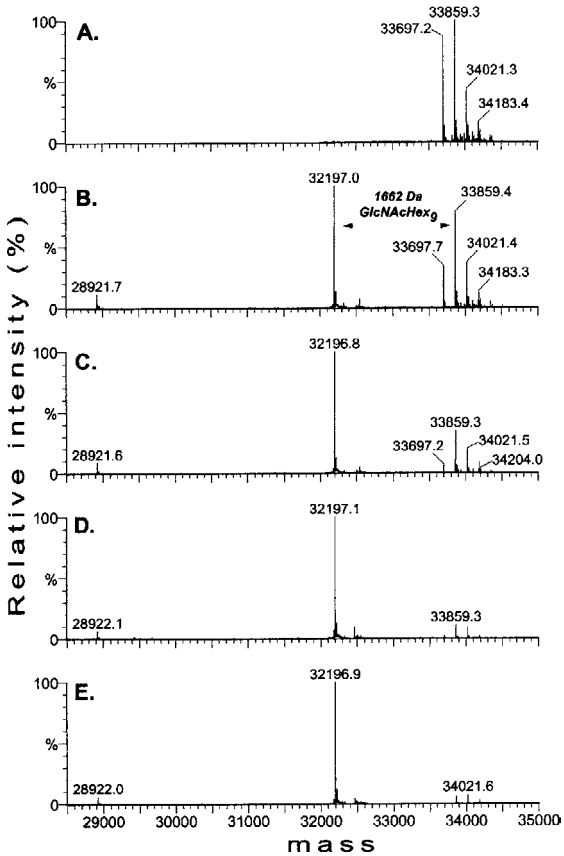

Figure 8 Reconstructed zero-charge spectra of the deglycosylation of recombinant BobXET16A by Endo H

Reaction time at 25 °C: (**A**) 0 min, (**B**) 15 min, (**C**) 35 min, (**D**) 60 min, (**E**) 114 min. The peak at 28922 in (**B**)–(**D**) is Endo H.

Endo H does not correlate with the value calculated from the publicly available Endo H protein sequence. Using external TOF calibration, we have previously obtained an average value of 28924 Da (results not shown). Although this value could be used to bring the observed mass of recombinant BobXET16A into closer agreement with the calculated value, the continuum spectra shown in Figure 8 are uncorrected.

The mass difference between the deglycosylated enzyme and the major glycoform observed by ESI/MS is 1662 Da. This value corresponds to the mass of a glycan of the general structure $GlcNAc_1Man_9$, which would be expected to be lost due to the Endo H-mediated cleavage of a high-mannose-type glycan. Careful inspection of the spectrum in Figure 8(A) indicates the presence of at least five enzyme glycoforms bearing high-mannose-type oligosaccharides with eight to twelve mannose units.

To determine the effect of N-linked glycosylation on enzyme activity, a time-course experiment was carried out in which ESI/MS analysis was used to quantify the extent of protein deglycosylation by Endo H while simultaneously assaying XET activity using the colorimetric assay. Due to the observed instability of cauliflower XET at temperatures above 35 °C (Figure 2B), both the Endo H treatment and the colorimetric assay were performed at 25 °C to help minimize any effect of decreased protein stability due to deglycosylation. The same range of ions of *m*/*z* 800–1600 was chosen for the MaxEnt1 processing of all MS spectra to avoid biasing reconstructed peak areas due to differences in the distribution of observed charge states between recombinant and

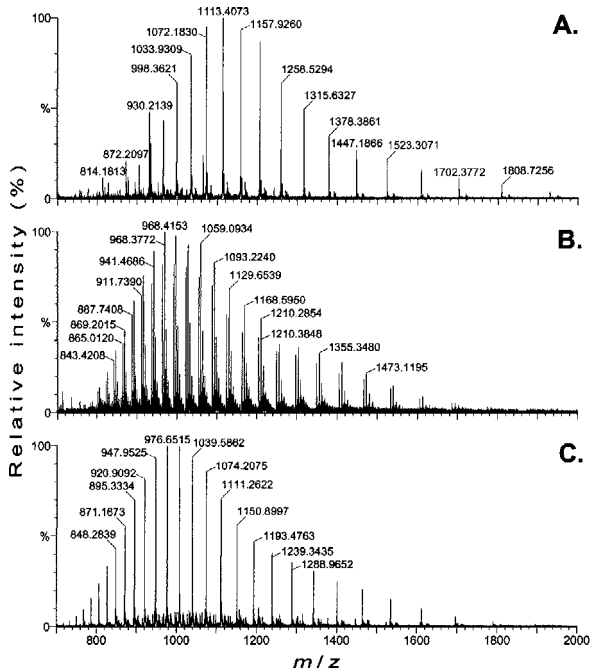

Figure 9 Combined individual spectra of Endo H (A), BobXET16A (B), and BobXET16A treated with Endo H for 150 min (C)

Data in the range *m/z* 800–1600 were used to produce MaxEnt1-reconstructed spectra in Endo H deglycosylation experiments.

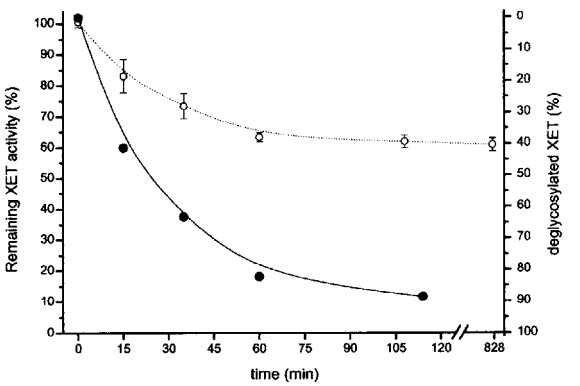

Figure 10 Endo H-mediated deglycosylation of recombinant BobXET16A

●, Percentage of deglycosylated BobXET16A, based upon peak-area fraction; ○, remaining XET activity (10 min assay at 25 °C). Error bars on activity mesurements represent S.D.s calculated from duplicate determinations. B-spline curves were drawn through the data points using Microcal™ Origin® v.6.0 to serve as ocular guides.

deglycosylated protein. As shown in Figure 9, this range included the majority of observed multiply charged ions arising from the ESI of Endo H, recombinant BobXET16A and deglycosylated BobXET16A.

Peak areas of the protein glycoforms over the course of the deglycosylation experiment were determined by the generation of centroid spectra from the MaxEnt1-reconstructed spectra shown in Figure 8. This allowed the extent of deglycosylation at each time point to be calculated directly as a percentage, based upon the peak-area fraction [defined as (peak area)/(sum of all peak areas considered)] of the deglycosylated enzyme (Figure 10). Peak areas for the major glycoforms at *m/z* 32197, 33697, 33859 and 34021 were included in the analysis, while less abundant peaks due to monosodiated adducts (+22 Da) of the different protein species were not considered in the calculations. Similar results were obtained when peak areas were normalized using the Endo H peak area as an internal standard, excluding the 0 min (no Endo H) spectrum (results not shown). The extent of deglycosylation during the course of the experiment was also determined by SDS/PAGE analysis (results not shown), the results of which were in good agreement with the MS results. When the percentage XET activity remaining over time is compared with the percentage deglycosylation of BobXET16, it is observed that the decrease in XET activity followed N-glycan removal (Figure 10). However, the loss of activity was not complete: with 90% deglycosylation, 60% of the original activity was maintained. The endo-xyloglucanase (hydrolytic) activity of the enzyme, which was less than 75 pmol · min^{-1} · mg^{-1} of enzyme (limit of detection of the BCA reducing-sugar assay), was unchanged at this level of deglycosylation. Similar results were obtained when a 4-fold greater amount of Endo H was used, except that the rates of deglycosylation and loss of activity were higher (results not shown).

It should be noted that the time values indicated in Figure 10 represent the times at which samples were withdrawn for each analysis, and that no attempt was made to abolish the activity of Endo H prior to assaying the sample for XET activity. Although Endo H has no detectable XET or endo-xyloglucanase activity at the concentrations used in this experiment (results not shown), the deglycosylation process would have continued during the duration of the 10 min XET assay (assuming no direct inhibition of Endo H activity by the XET assay conditions). However, the rate of deglycosylation during this time was probably greatly reduced, due to the dilution of Endo H and XET by a factor of 1:40 in the assay mixture. It is therefore likely that the MS data accurately reflect the glycosylation state of the XET in the assay. By comparison, samples for MS analysis were diluted immediately in acetonitrile/water (1:1, v/v) containing 0.1% formic acid, and spectral acquisition was completed in under 3 min.

DISCUSSION

Protein glycosylation in certain XET enzymes has been shown previously to affect enzyme activity dramatically [40,41]. In the present work, a detailed analysis of the glycosylation of cauliflower XET16A was carried out in order to better define the structure of the N-linked glycan and to confirm its attachment to the conserved Asn-Xaa-Thr motif close to the predicted active-site residues (Glu-85 and Glu-89; Figure 7).

To obtain protein for this work, a new purification strategy to obtain cauliflower XET was developed. Two highly specific XET purification strategies have been presented previously that rely upon the formation of a tightly bound, presumably covalent, xyloglucan–XET intermediate [36,50]. Although conceptually elegant, these methods suffer from certain limitations with respect to scale-up, either because significant amounts of XGO must be used to release complexed XET, or because the amount of chromatographic matrix required for larger purifications becomes unwieldy. In order to obtain cauliflower XET in quantities suitable for protein crystallographic studies and biotechnological applications, we therefore sought to develop an easily scalable method for XET purification based upon classical protein purification techniques. The batch adsorption of XET on to cation-exchange resin as a first step in the purification was particularly advantageous, as it both eliminated the losses associated with

ammonium sulphate precipitation/redissolution in our hands and greatly eased the removal of debris resulting from the homogenization of plant material. Despite the fact that XET activity was eluted in a rather broad peak from this column, the subsequent hydrophobic-interaction chromatography step produced a single glycoform of cauliflower XET in good yield relative to literature methods [36,39].

For practical reasons, we routinely used the colorimetric assay of Farkaš and co-workers [47], but also employed the radioactive assay of Fry and co-workers [39] when preparing enzyme purification tables. It is noteworthy that the two methods gave rise to different purification factors (fold purification values) throughout the purification. We have observed this phenomenon in the purification of XET enzymes from different sources in our laboratory, but, to our knowledge, there are no reports describing a comparative study of the two assays. Although both assays measure the incorporation of short XGO (1060–1390 Da) into high-molecular-mass xyloglucan ($\approx$200000 Da) by transglycosylation, the analytical methods are fundamentally different. The colorimetric assay relies upon the formation of a blue–green complex between xyloglucan and I_3^- under conditions of high ionic strength, which is believed to require xyloglucan molecules larger than 10000 Da [47]. This assay therefore measures an average shift in the molecular mass of a population of xyloglucan molecules, and does not measure individual catalytic events. Furthermore, any substance that interferes with tri-iodide complex formation may affect the accuracy of the measurements. In contrast, the radioactive assay measures the direct incorporation of a ^{3}H-labelled nonasaccharide into soluble xyloglucan, which is subsequently trapped by adsorption on cellulose filter paper [3,36,39]. The binding of xyloglucan to cellulose is largely pH-independent, but requires a backbone of approximately 16 glucose units [51], so the unincorporated radiolabelled acceptor may be conveniently washed away with water. While it is to be expected that the absolute values of the assays will not be comparable due to these experimental differences, it is difficult to reconcile the different purification factors obtained, since the effect of a systematic error in either assay should be eliminated when the specific-activity data are normalized (Table 2). However, we place more trust in the purification data obtained with the radioactive assay, both because it is a more direct measure of enzymic transglycosylation and because there is a greater chance for impurities in early stages of the purification to interfere with the colorimetric assay.

Cauliflower XET isoforms have been characterized extensively with respect to their catalytic activities [17,39]. Basic characterization data indicate that the native cauliflower XET16A exhibits limited thermal stability, similar to that described previously for a range of isoforms [39]. Additionally, the pH–rate profile (Figure 2B) is strikingly similar to that determined by Steele and Fry [39] for isoenzyme C30, including the rapid, non-sigmoidal decrease in activity below pH 5.0. In the absence of sequence information for isoenzyme C30, however, it is unclear whether this isoenzyme and BobXET16A are the same protein.

At present, there is no publicly available sequence information on XET-related proteins from cauliflower (or any other *B. oleracea* varieties), despite the extensive and detailed enzymological studies that have been carried out on XET isoforms from this source. In contrast, XET-related genes from other plant species, especially *Arabidopsis thaliana*, have received much attention with regard to sequence and expression analysis, but comparatively little is known about the catalytic characteristics of the gene products. To help bridge this gap, isolation of the cDNA encoding the purified cauliflower XET was accomplished from initial N-terminal sequence information coupled with sequence alignment of known GH16 XET-related proteins. The isolated cauliflower XET, BobXET16A, was nearly identical with EXGT-A1 (EXGT, XTH4) from *A. thaliana* [5] (96 % at the amino acid level), which places BobXET16A into subfamily I. Cauliflower is a variety of *Brassica oleracea* that results from a hyperproliferation of meristematic tissue. Interestingly, cauliflower XET16A shares only 53 % protein sequence identity with *A. thaliana* Meri-5 XET (XTH24) of subfamily II, which was originally isolated from meristematic tissue using cauliflower meristematic cDNA as a probe [52]. It has been speculated that gene subfamily classification may be used to predict hydrolytic compared with transglycosylation activity [53], but the observation of XET enzymes with hydrolytic activity in different subfamilies casts doubt on this hypothesis [1,32–34]. Through the heterologous expression of BobXET16A, we were able to produce this enzyme in a manner that guaranteed that there were no contaminating plant-derived endoglucanase activities present. Comparison of the rate of hydrolysis of xyloglucan in the absence of added acceptor substrates (undetectable; <75 pmol $\cdot$ min^{-1} $\cdot$ mg^{-1}) and the rate of XLLGol incorporation into xyloglucan by transglycosylation (812 nmol $\cdot$ min^{-1} $\cdot$ mg^{-1}; Table 2) indicates that this enzyme is a strict transglycosylase. The ratio of transglycosylation rate to hydrolysis rate of 11000 thus represents a lower limit, since the amount of free reducing ends produced by hydrolysis was below the detection limit of the BCA reducing-sugar assay. Furthermore, calculation of the transglycosylation rate is based upon a published ^{3}H counting efficiency of xyloglucan bound to cellulose filter papers of 44 % [3]. Generally, ^{3}H counting efficiency from cellulose filters is low (1–4 %) and difficult to determine precisely [54,55], so the transglycosylation rate may be underestimated by over an order of magnitude.

MS studies on native and enzymically deglycosylated cauliflower XET confirmed that the protein isolated from cauliflower florets was the product of translation of the *BobXET16A* gene. The intact protein mass obtained for the native protein by ESI/MS analysis following PNGase F treatment correlated with the mass calculated from the translated cDNA sequence. Peptide sequencing by classical N-terminal Edman degradation and MS/MS analysis further confirmed the relationship between the protein and the cloned cDNA sequence. The protein sequence coverage obtained by MS/MS analysis was quite high (over 60 %), although we did not pursue every predicted tryptic peptide exhaustively. Similar studies using a Q-Tof™ mass spectrometer have shown that it is possible to obtain sequence coverage of over 90 %, and that a combination of accurate peptide and intact protein mass data can be correlated directly with genetic sequence information [56].

Comparison of the predicted protein mass with those observed for untreated and deglycosylated cauliflower XET protein, either from the native source or expressed heterologously, allowed us to determine directly the glycoform composition of enzyme preparations. Although ESI/MS is unable to provide the same level of structural detail as exhaustive analysis using a combination of methods (e.g. HPLC, NMR, MS and multiple glycosidase digestion), this technique can very rapidly provide an overview of the nature and extent of N-glycan diversity in a sample when general protein glycosylation pathways are considered. The initial steps of protein N-glycosylation are identical in plants [57] and yeast [58], beginning in the endoplasmic reticulum with the transfer of a $Glc_3Man_9GlcNAc_2$ moiety from a dolichol pyrophosphate carrier to an asparagine residue in the consensus motif Asn-Xaa-Ser/Thr [59]. Further processing in the endoplasmic reticulum then occurs due to the action of specific glucosidases to yield a $Man_9GlcNAc_2$ structure. In many yeasts, including

Pichia pastoris, this structure is trimmed further in the endoplasmic reticulum by the action of an $\alpha(1 \rightarrow 2)$-mannosidase to give $Man_8GlcNAc_2$, prior to transfer of the nascent glycoprotein to the Golgi apparatus. In contrast, a similar activity has not been found in plants, which pass the $Man_9GlcNAc_2$ glycan to the Golgi unchanged. Once in the Golgi, the glycan structure in both plants and yeast may be modified further in a species-dependent fashion. In *P. pastoris*, the core structure is extended by the addition of a limited number of Man residues to produce $Man_{8-11}GlcNAc_2$ glycans of known structure. *P. pastoris* can also produce larger phosphomannans whose structure is less well characterized [58]. Although the structure of cauliflower N-glycans has not been studied in detail, plants, in general, are capable of a wider array of glycan modification than *P. pastoris*. Within the plant Golgi, an $\alpha(1 \rightarrow 2)$-mannosidase (α-Man I) can trim the core glycan down to structures as small as $Man_5GlcNAc_2$ prior to construction of complex- and paucimannosidic-type glycans. Key features of these glycans include $\alpha(1 \rightarrow 3)$-fucosylation of the Asn-linked core GlcNAc, core xylosidation, and decoration of the glycan antennae with galactose, *N*-acetylglucosamine and fucose [57,60].

MS and MS/MS data for the native and PNGase F-treated cauliflower XET indicated that the sugar composition of the N-glycan is $GlcNAc_2Hex_6$. Based upon the known plant core glycan structure and the mode of action of $\alpha(1 \rightarrow 2)$-mannosidase in the Golgi [57], a likely structure for the cauliflower XET glycan is Man(α1-6)[Man(α1-3)]Man(α1-6)[Man(α1-3)]Man(β1-4)GlcNAc(β1-4)GlcNAc (IUPAC condensed notation) bearing an additional $\alpha(1 \rightarrow 2)$-linked Man on one of the three terminal Man residues [60]. Core fucosylation of the glycan was not indicated due to the sensitivity of the glycoprotein to PNGase F, which does not cleave complex-type glycopeptides bearing Fuc on the first core GlcNAc. Furthermore, the presence of Xyl or Fuc on the core and GlcNAc or Fuc on the antennae was not supported by the protein MS and glycopeptide MS/MS data. No evidence for the neutral loss of these monosaccharides was observed from the MS/MS spectrum of the glycopeptide (Figure 5). Additionally, the glycan mass determined from TOF-MS data for the native and PNGase F-treated enzyme (Figure 3) could not be rectified with calculated masses based on combinations of these sugars.

TOF-MS data acquired with recombinant BobXET16A both before and after treatment with Endo H (Figure 8) indicated that this preparation most probably contained only high-mannose-type N-glycans with the general composition $Man_{8-12}GlcNAc_2$. As with the native enzyme, structures bearing further modifications, e.g. non-hexose sugars or phosphate groups, were not observed. This degree of glycosylation is commonly observed in proteins from *P. pastoris*, and it is likely that the glycan structures of BobXET16A are similar to those found in other proteins produced in this host [58,61]. BobXET16A produced in *P. pastoris* is slightly more heavily glycosylated than the glycoform isolated from the native source, which bears six mannose units. However, this differential glycosylation does not seem to have a large effect on the specific activity of the enzyme, which was similar in the two samples.

MS analysis at the peptide level allowed the demonstration, for the first time, that the putative N-linked glycosylation site found in the majority of XET-related protein sequences is in fact the site of glycan attachment. The proximity of this site to the conserved GH16 catalytic residues has been noted at the protein sequence level, and crystallographic data indicate that the putative glycosylation site is located near the acceptor binding end (positive subsites) of the enzyme active-site cleft [42]. The effect of glycosylation on enzyme mechanism has not been studied extensively, although there is some evidence that glycosylation can influence enzyme reaction rates through dynamic effects [62] or by specific interaction with the active site [63]. It has been observed previously that the removal of glycosylation in recombinant *A. thaliana* TCH4 and Meri-5 XET enzymes by PNGase F abolished $>95\%$ of the XET activity, while deglycosylation of TCH4 with Endo H caused only a partial loss of activity (48%) [40,41]. However, these deglycosylation reactions were conducted using a prolonged incubation time (2 h) at a temperature (37 °C) at which the recombinant enzyme already shows decreased stability [40], so it is unclear whether the effect on activity was due to increased enzyme instability or mechanistic effects. Therefore, based upon data for the native cauliflower enzyme (Figure 2), a lower temperature (25 °C) and a pH close to the activity optimum (5.5) were used in both the deglycosylation reaction and the colorimetric XET assay to maximize stability. ESI-MS proved to be a useful technique for quantifying the extent of glycan removal over time, which allowed these data to be correlated directly with a loss of XET activity (Figure 10). Interestingly, the enzyme retained over 60% of the original transglycosylating activity and showed no appearance of hydrolytic activity when 90% deglycosylated. These data imply that the catalytic mechanism of cauliflower XET16A is not strictly dependent on the presence of the glycan, and that the glycan does not affect the ratio of substrate transglycosylation to hydrolysis. It has been shown previously that a tomato fruit XET, which was expressed in a denatured form in *Escherichia coli* (thus lacking an N-glycan), could be refolded successfully to produce an enzyme with transglycosylating, but not hydrolytic, activity [64]. However, it is not known whether this enzyme is glycosylated in the native source, although it does contain the conserved N-glyosylation motif close to the predicted active-site residues. Curiously, it has been reported that EXGT (also known as EXGT-A1 or XTH4) [5], which shares 96% peptide sequence identity with BobXET16A, retained 91% activity after complete deglycosylation with PNGase F at 37 °C [40]. This activity was reported relative to that in a mock-treated sample, which lacked PNGase F but was maintained similarly in 50 mM sodium phosphate, pH 7.5, at 37 °C for 2 h. It was not stated whether this sample retained the activity of the original enzyme preparation, so it is unclear if both samples lost activity, although to a similar extent. In the present study, the control sample lacking Endo H essentially retained full activity relative to the enzyme stock, so the data in Figure 10 represent true activity losses resulting from the deglycosylation reaction. Further detailed structural and biophysical studies will clearly be required to elucidate the precise contributions of the glycan to catalysis and enzyme stability in both BobXET16A and other XET homologues.

This work was generously supported by the Knut and Alice Wallenberg Foundation. The purchase of MS equipment at KTH was financed by the Wallenberg Consortium North for Functional Genomics. We thank Mr Thorleif Lavold (Waters Corp., Micromass MS Technologies, Sweden) for facilitating the collaboration between the KTH group and Waters Corporation, Micromass MS Technologies. We thank Iria Fernandez for help with gene cloning, Martin Baumann for optimizing XGO preparation and analysis, and Åsa Kallas for assistance with the radioactive XET assay.

REFERENCES

1 Edwards, M., Dea, I. C. M., Bulpin, P. V. and Reid, J. S. G. (1986) Purification and properties of a novel xyloglucan-specific endo-(1 → 4)-beta-D-glucanase from germinated nasturtium seeds (*Tropaeolum majus* L). J. Biol. Chem. **261**, 9489–9494

2 McDougall, G. J. and Fry, S. C. (1990) Xyloglucan oligosaccharides promote growth and activate cellulase – evidence for a role of cellulase in cell expansion. Plant Physiol. **93**, 1042–1048

3 Fry, S. C., Smith, R. C., Renwick, K. F., Martin, D. J., Hodge, S. K. and Matthews, K. J. (1992) Xyloglucan endotransglycosylase, a new wall-loosening enzyme activity from plants. Biochem. J. **282**, 821–828
4 Nishitani, K. and Tominaga, R. (1992) Endoxyloglucan transferase, a novel class of glycosyltransferase that catalyzes transfer of a segment of xyloglucan molecule to another xyloglucan molecule. J. Biol. Chem. **267**, 21058–21064
5 Okazawa, K., Sato, Y., Nakagawa, T., Asada, K., Kato, I., Tomita, E. and Nishitani, K. (1993) Molecular cloning and cDNA sequencing of endoxyloglucan transferase, a novel class of glycosyltransferase that mediates molecular grafting between matrix polysaccharides in plant cell walls. J. Biol. Chem. **268**, 25364–25368
6 de Silva, J., Jarman, C. D., Arrowsmith, D. A., Stronach, M. S., Chengappa, S., Sidebottom, C. and Reid, J. S. G. (1993) Molecular characterization of a xyloglucan-specific endo-(1 → 4)-beta-D-glucanase (xyloglucan endotransglycosylase) from nasturtium seeds. Plant J. **3**, 701–711
7 Vincken, J. P., York, W. S., Beldman, G. and Voragen, A. G. J. (1997) Two general branching patterns of xyloglucan, XXXG and XXGG. Plant Physiol. **114**, 9–13
8 Vierhuis, E., York, W. S., Kolli, V. S. K., Vincken, J. P., Schols, H. A., Van Alebeek, G. and Voragen, A. G. J. (2001) Structural analyses of two arabinose containing oligosaccharides derived from olive fruit xyloglucan: XXSG and XLSG. Carbohydr. Res. **332**, 285–297
9 Whitney, S. E. C., Gothard, M. G. E., Mitchell, J. T. and Gidley, M. J. (1999) Roles of cellulose and xyloglucan in determining the mechanical properties of primary plant cell walls. Plant Physiol. **121**, 657–663
10 Pauly, M., Albersheim, P., Darvill, A. and York, W. S. (1999) Molecular domains of the cellulose/xyloglucan network in the cell walls of higher plants. Plant J. **20**, 629–639
11 Rose, J. K. C. and Bennett, A. B. (1999) Cooperative disassembly of the cellulose-xyloglucan network of plant cell walls: parallels between cell expansion and fruit ripening. Trends Plant Sci. **4**, 176–183
12 Brummell, D. A. and Harpster, M. H. (2001) Cell wall metabolism in fruit softening and quality and its manipulation in transgenic plants. Plant Mol. Biol. **47**, 311–340
13 Campbell, P. and Braam, J. (1999) Xyloglucan endotransglycosylases: diversity of genes, enzymes and potential wall-modifying functions. Trends Plant Sci. **4**, 361–366
14 Pauly, M., Qin, Q., Greene, H., Albersheim, P., Darvill, A. and York, W. S. (2001) Changes in the structure of xyloglucan during cell elongation. Planta **212**, 842–850
15 Baran, R., Sulová, Z., Stratilova, E. and Farkaš, V. (2000) Ping-pong character of nasturtium-seed xyloglucan endotransglycosylase (XET) reaction. Gen. Physiol. Biophys. **19**, 427–440
16 Lorences, E. P. and Fry, S. C. (1993) Xyloglucan oligosaccharides with at least 2 alpha-D-xylose residues act as acceptor substrates for xyloglucan endotransglycosylase and promote the depolymerization of xyloglucan. Physiol. Plant. **88**, 105–112
17 Steele, N. M., Sulová, Z., Campbell, P., Braam, J., Farkaš, V. and Fry, S. C. (2001) Ten isoenzymes of xyloglucan endotransglycosylase from plant cell walls select and cleave the donor substrate stochastically. Biochem. J. **355**, 671–679
18 Sulová, Z. and Farkaš, V. (1998) Kinetic evidence of the existence of a stable enzyme-glycosyl intermediary complex in the reaction catalyzed by endotransglycosylase. Gen. Physiol. Biophys. **17**, 133–142
19 Sulová, Z., Takacova, M., Steele, N. M., Fry, S. C. and Farkaš, V. (1998) Xyloglucan endotransglycosylase: evidence for the existence of a relatively stable glycosyl-enzyme intermediate. Biochem. J. **330**, 1475–1480
20 Vissenberg, K., Martinez-Vilchez, I. M., Verbelen, J. P., Miller, J. G. and Fry, S. C. (2000) *In vivo* colocalization of xyloglucan endotransglycosylase activity and its donor substrate in the elongation zone of arabidopsis roots. Plant Cell **12**, 1229–1237
21 Vissenberg, K., Fry, S. C. and Verbelen, J. P. (2001) Root hair initiation is coupled to a highly localized increase of xyloglucan endotransglycosylase action in arabidopsis roots. Plant Physiol. **127**, 1125–1135
22 Ito, H. and Nishitani, K. (1999) Visualization of EXGT-mediated molecular grafting activity by means of a fluorescent-labeled xyloglucan oligomer. Plant Cell Physiol. **40**, 1172–1176
23 Thompson, J. E., Smith, R. C. and Fry, S. C. (1997) Xyloglucan undergoes interpolymeric transglycosylation during binding to the plant cell wall *in vivo*: Evidence from C-13/H-3 dual labelling and isopycnic centrifugation in caesium trifluoroacetate. Biochem. J. **327**, 699–708
24 Thompson, J. E. and Fry, S. C. (2001) Restructuring of wall-bound xyloglucan by transglycosylation in living plant cells. Plant J. **26**, 23–34
25 Bourquin, V., Nishikubo, N., Abe, H., Brumer, H., Denman, S., Eklund, M., Christiernin, M., Teeri, T. T., Sundberg, B. and Mellerowicz, E. J. (2002) Xyloglucan endotransglycosylases have a function during the formation of secondary cell walls of vascular tissues. Plant Cell **14**, 3073–3088
26 Rose, J. K. C., Brummell, D. A. and Bennett, A. B. (1996) Two divergent xyloglucan endotransglycosylases exhibit mutually exclusive patterns of expression in nasturtium. Plant Physiol. **110**, 493–499
27 Aubert, D. and Herzog, M. (1996) A new cDNA encoding a xyloglucan endo-transglycosylase-related polypeptide (AtXTR8) preferentially expressed in seedling, root and stem of *Arabidopsis thaliana*. Plant Sci. **121**, 187–196
28 Catala, C., Rose, J. K. C., York, W. S., Albersheim, P., Darvill, A. G. and Bennett, A. B. (2001) Characterization of a tomato xyloglucan endotransglycosylase gene that is down-regulated by auxin in etiolated hypocotyls. Plant Physiol. **127**, 1180–1192
29 Yokoyama, R. and Nishitani, K. (2001) A comprehensive expression analysis of all members of a gene family encoding cell-wall enzymes allowed us to predict cis-regulatory regions involved in cell-wall construction in specific organs of *Arabidopsis*. Plant Cell Physiol. **42**, 1025–1033
30 Henrissat, B. and Davies, G. (1997) Structural and sequence-based classification of glycoside hydrolases. Curr. Opin. Struct. Biol. **7**, 637–644
31 Davies, G., Sinnott, M. L. and Withers, S. G. (1997) Glycosyl transfer. In Comprehensive Biological Catalysis, vol. I (Sinnott, M. L., ed.), pp. 119–208, Academic Press, London
32 Schröder, R., Atkinson, R. G., Langenkamper, G. and Redgwell, R. J. (1998) Biochemical and molecular characterisation of xyloglucan endotransglycosylase from ripe kiwifruit. Planta **204**, 242–251
33 Tabuchi, A., Mori, H., Kamisaka, S. and Hoson, T. (2001) A new type of endo-xyloglucan transferase devoted to xyloglucan hydrolysis in the cell wall of azuki bean epicotyls. Plant Cell Physiol. **42**, 154–161
34 Tabuchi, A., Kamisaka, S. and Hoson, T. (1997) Purification of xyloglucan hydrolase/endotransferase from cell walls of azuki bean epicotyls. Plant Cell Physiol. **38**, 653–658
35 Rose, J. K. C., Braam, J., Fry, S. C. and Nishitani, K. (2002) The XTH family of enzymes involved in xyloglucan endotransglucosylation and endohydrolysis: current perspectives and a new unifying nomenclature. Plant Cell Physiol. **43**, 1421–1435
36 Steele, N. M. and Fry, S. C. (1999) Purification of xyloglucan endotransglycosylases (XETs): a generally applicable and simple method based on reversible formation of an enzyme-substrate complex. Biochem. J. **340**, 207–211
37 Fry, S. C. (1997) Novel 'dot-blot' assays for glycosyltransferases and glycosylhydrolases: Optimization for xyloglucan endotransglycosylase (XET) activity. Plant J. **11**, 1141–1150
38 Iannetta, P. P. M. and Fry, S. C. (1999) Visualization of the activity of xyloglucan endotransglycosylase (XET) isoenzymes after gel electrophoresis. Phytochem. Anal. **10**, 238–240
39 Steele, N. M. and Fry, S. C. (2000) Differences in catalytic properties between native isoenzymes of xyloglucan endotransglycosylase (XET). Phytochemistry **54**, 667–680
40 Campbell, P. and Braam, J. (1999) *In vitro* activities of four xyloglucan endotransglycosylases from *Arabidopsis*. Plant J. **18**, 371–382
41 Campbell, P. and Braam, J. (1998) Co- and/or post-translational modifications are critical for TCH4 XET activity. Plant J. **15**, 553–561
42 Johansson, P., Denman, S., Brumer, H., Kallas, A. M., Henriksson, H., Bergfors, T., Teeri, T. T. and Jones, T. A. (2003) Crystallization and preliminary X-ray analysis of a xyloglucan endotransglycosylase from *Populus tremula x tremuloides*. Acta Crystallogr. D Biol. Crystallogr. **59**, 535–537
43 Henrissat, B., Teeri, T. T. and Warren, R. A. J. (1998) A scheme for designating enzymes that hydrolyse the polysaccharides in the cell walls of plants. FEBS Lett. **425**, 352–354
44 Morrissey, J. H. (1981) Silver stain for proteins in polyacrylamide gels – a modified procedure with enhanced uniform sensitivity. Anal. Biochem. **117**, 307–310
45 Vincken, J. P., Beldman, G. and Voragen, A. G. J. (1997) Substrate specificity of endoglucanases: What determines xyloglucanase activity? Carbohydr. Res. **298**, 299–310
46 Fry, S. C., York, W. S., Albersheim, P., Darvill, A., Hayashi, T., Joseleau, J. P., Kato, Y., Lorences, E. P., Maclachlan, G. A., McNeil, M. et al. (1993) An unambiguous nomenclature for xyloglucan-derived oligosaccharides. Physiol. Plant. **89**, 1–3
47 Sulová, Z., Lednicka, M. and Farkaš, V. (1995) A colorimetric assay for xyloglucan endotransglycosylase from germinating seeds. Anal. Biochem. **229**, 80–85
48 Garcia, E., Johnston, D., Whitaker, J. R. and Shoemaker, S. P. (1993) Assessment of endo-1,4-beta-D-glucanase activity by a rapid colorimetric assay using disodium 2,2′-bicinchoninate. J. Food Biochem. **17**, 135–145
49 Perkins, D. N., Pappin, D. J. C., Creasy, D. M. and Cottrell, J. S. (1999) Probability-based protein identification by searching sequence databases using mass spectrometry data. Electrophoresis **20**, 3551–3567
50 Sulová, Z. and Farkaš, V. (1999) Purification of xyloglucan endotransglycosylase based on affinity sorption of the active glycosyl-enzyme intermediate complex to cellulose. Protein Expression Purif. **16**, 231–235
51 Vincken, J. P., de Keizer, A., Beldman, G. and Voragen, A. G. J. (1995) Fractionation of xyloglucan fragments and their interaction with cellulose. Plant Physiol. **108**, 1579–1585

52 Medford, J. I., Elmer, J. S. and Klee, H. J. (1991) Molecular cloning and characterization of genes expressed in shoot apical meristems. Plant Cell **3**, 359–370
53 Yokoyama, R. and Nishitani, K. (2000) Functional diversity of xyloglucan-related proteins and its implications in the cell wall dynamics in plants. Plant Biol. **2**, 598–604
54 Gill, D. M. (1967) Liquid scintillation counting of tritiated compounds supported by solid filters. Int. J. Appl. Radiat. Isot. **18**, 393–398
55 Brandsome, E. D. and Grower, M. F. (1970) Liquid scintillation counting of H-3 and C-14 on solid supports: a warning. Anal. Biochem. **38**, 401–408
56 Jonsson, A. P., Carlquist, M., Husman, B., Ljunggren, J., Jornvall, H., Bergman, T. and Griffiths, W. J. (1999) Structural analysis of the thyroid hormone receptor ligand binding domain: studies using a quadrupole time-of-flight tandem mass spectrometer. Rapid Commun. Mass Spectrom. **13**, 1782–1791
57 Rayon, C., Lerouge, P. and Faye, L. (1998) The protein N-glycosylation in plants. J. Exp. Bot. **49**, 1463–1472
58 Gemmill, T. R. and Trimble, R. B. (1999) Overview of N- and O-linked oligosaccharide structures found in various yeast species. Biochim. Biophys. Acta **1426**, 227–237
59 Gavel, Y. and von Heijne, G. (1990) Sequence differences between glycosylated and nonglycosylated Asn-X-Thr/Ser acceptor sites – implications for protein engineering. Protein Eng. **3**, 433–442
60 Bardor, M., Faye, L. and Lerouge, P. (1999) Analysis of the N-glycosylation of recombinant glycoproteins produced in transgenic plants. Trends Plant Sci. **4**, 376–380
61 Montesino, R., Garcia, R., Quintero, O. and Cremata, J. A. (1998) Variation in N-linked oligosaccharide structures on heterologous proteins secreted by the methylotrophic yeast *Pichia pastoris*. Protein Expression Purif. **14**, 197–207
62 Kohen, A., Jonsson, T. and Klinman, J. P. (1997) Effects of protein glycosylation on catalysis: changes in hydrogen tunneling and enthalpy of activation in the glucose oxidase reaction. Biochemistry **36**, 2603–2611
63 Lloyd, R. C., Davis, B. G. and Jones, J. B. (2000) Site-selective glycosylation of subtilisin *Bacillus lentus* causes dramatic increases in esterase activity. Bioorg. Med. Chem. **8**, 1537–1544
64 Arrowsmith, D. A. and de Silva, J. (1995) Characterization of two tomato fruit-expressed cDNAs encoding xyloglucan endo-transglycosylase. Plant Mol. Biol. **28**, 391–403

Received 31 March 2003/2 June 2003; accepted 25 June 2003
Published as BJ Immediate Publication 26 June 2003, DOI 10.1042/BJ20030485